Control of Kir channel gating by cytoplasmic domain interface interactions

William F. Borschel,[1,2] Shizhen Wang,[1,2] Sunjoo Lee,[1,2] and Colin G. Nichols[1,2]

[1]Department of Cell Biology and Physiology and [2]Center for the Investigation of Membrane Excitability Diseases, Washington University School of Medicine, St. Louis, MO 63110

Inward rectifier potassium (Kir) channels are expressed in almost all mammalian tissues and play critical roles in the control of excitability. Pancreatic ATP-sensitive K (K_{ATP}) channels are key regulators of insulin secretion and comprise Kir6.2 subunits coupled to sulfonylurea receptors. Because these channels are reversibly inhibited by cytoplasmic ATP, they link cellular metabolism with membrane excitability. Loss-of-function mutations in the pore-forming Kir6.2 subunit cause congenital hyperinsulinism as a result of diminished channel activity. Here, we show that several disease mutations, which disrupt intersubunit salt bridges at the interface of the cytoplasmic domains (CD-I) of adjacent subunits, induce loss of channel activity via a novel channel behavior: after ATP removal, channels open but then rapidly inactivate. Re-exposure to inhibitory ATP causes recovery from this inactivation. Inactivation can be abolished by application of phosphatidylinositol-4,5-bisphosphate (PIP_2) to the cytoplasmic face of the membrane, an effect that can be explained by a simple kinetic model in which PIP_2 binding competes with the inactivation process. Kir2.1 channels contain homologous salt bridges, and we find that mutations that disrupt CD-I interactions in Kir2.1 also reduce channel activity and PIP_2 sensitivity. Kir2.1 channels also contain an additional CD-I salt bridge that is not present in Kir6.2 channels. Introduction of this salt bridge into Kir6.2 partially rescues inactivating mutants from the phenotype. These results indicate that the stability of the intersubunit CD-I is a major determinant of the inactivation process in Kir6.2 and may control gating in other Kir channels.

INTRODUCTION

Inward rectifier potassium (Kir) channels are phospholipid-gated, tetrameric protein complexes that are crucial in membrane potential control in various tissues, including the brain, heart, pancreas, and skeletal and smooth muscle (Nichols and Lopatin, 1997). Seven distinct Kir channel subunit families (Kir1–7) differ in their biophysical properties, sensitivity to phospholipids, organ distribution, and cellular localization (Hibino et al., 2010). Each Kir subunit consists of intracellular N- and C-terminal domains, two transmembrane helixes (TM1 and TM2), and a potassium-selective pore loop (Bichet et al., 2003). The ATP-sensitive Kir (K_{ATP}) channel complex is unique in requiring four sulfonylurea receptor (SURX) subunits in addition to the four pore forming Kir6.x subunits (Inagaki et al., 1995, 1996; Shyng and Nichols, 1997). All eukaryotic Kir channels require binding of phosphatidylinositol-4,5-bisphosphate (PIP_2) for activation (Huang et al., 1998; Shyng and Nichols, 1998; Zhang et al., 1999). In addition, ATP binding to the Kir6.x subunit inhibits K_{ATP} channels, whereas SURX subunits are responsible for MgADP activation and pharmacological modulation (Nichols et al., 1996; Gribble et al., 1997; Shyng et al., 1997b; Drain et al., 1998).

In WT Kir6.2 plus SUR1 K_{ATP} channels, removal of ATP from the cytoplasmic face results in a maintained channel opening. However, an early study attempting to identify positively charged Kir6.2 residues involved in PIP_2 binding revealed three intracellular arginine residues that, when mutated to alanine (R192A, R301A, and R314A), all resulted in channel activation after removal of intracellular ATP but then rapid channel closure (Shyng et al., 2000). This phenomenon was termed "inactivation" as channel activity reappeared (and again decayed) after subsequent application and removal of ATP. In a follow-up study (Lin et al., 2003), it was shown that individual R314E/C or E229R/C mutations also induced an inactivation phenotype, whereas double charge reversal (R314E/E229R) or double cysteine substitutions (R314C/E229C) reverted to a noninactivating behavior. R314 and E229 map to the intersubunit cytoplasmic domain interface (CD-I), suggesting that salt bridge–induced stability of this interface might normally be important for maintenance of channel activity.

Pancreatic K_{ATP} channels composed of Kir6.2/SUR1 subunits are active during low metabolic conditions, keeping the β cell membrane hyperpolarized and inhibiting insulin secretion (Nichols and Remedi, 2012).

Correspondence to Colin G. Nichols: cnichols@wustl.edu

Abbreviations used: CD-I, cytoplasmic domain interface; GFP, green fluorescent protein; HI, hyperinsulinism; iGluR, ionotropic glutamate receptor; Kir, inward rectifier potassium; LBD, ligand-binding domain; LOF, loss-of-function; MOT, mean open time; PIP_2, phosphatidylinositol-4,5-bisphosphate; PL, phospholipid.

The Rockefeller University Press $30.00
J. Gen. Physiol. 2017 Vol. 149 No. 5 561–576
https://doi.org/10.1085/jgp.201611719

Gain-of-function mutations in either Kir6.2 or SUR1 result in maintained β cell hyperpolarization, leading to inhibition of insulin secretion, and neonatal diabetes mellitus (Koster et al., 2000; Gloyn et al., 2004). Conversely, loss-of-function (LOF) mutations result in maintained β cell electrical activity and hyperinsulinism (HI; Nichols et al., 1996). LOF in such mutations can result from decreased surface expression through deficits in protein production and membrane trafficking but can also arise from decreased channel activity (Koster et al., 2002; Remedi et al., 2006; Loechner et al., 2011; Martin et al., 2013). Several such HI-linked Kir6.2 LOF mutations (Shyng et al., 2012) reduce channel activity by inducing an inactivating behavior. The majority of these mutations are located at the CD-I and are predicted to disrupt salt bridge contacts between subunits, suggesting that disruption of CD-I interactions might be the molecular mechanism responsible for the inactivation and ultimately the disease phenotype (Lin et al., 2008, 2013; Shimomura et al., 2009; Bushman et al., 2010, 2013; Loechner et al., 2011).

This inactivation phenomenon has only been identified in Kir6.2-containing K_{ATP} channels. In this study, we set out to further examine the underlying molecular mechanism and to consider the possibility that manipulation of the CD-I stability may affect gating in other Kir channels.

MATERIALS AND METHODS

Molecular biology and heterologous expression system

Cosm6 cells were grown in Dulbecco's modified Eagle's medium supplemented with 10% fetal bovine serum and 1% penicillin/streptomycin in 95% O_2/5% CO_2 at 37°C. Cells between passages 10 and 30 were plated on glass coverslips in 40-mm, 6-well plates. At 30–50% confluency, cells were transiently transfected with plasmids in pcDNA3.1 encoding either mouse Kir6.2 (mKir6.2) and hamster SUR1, or human Kir2.1 (hKir2.1), along with green fluorescent protein (GFP) using Fugene6 (Promega). Each well was transfected with 0.2 µg GFP and either 0.3 µg mKir6.2 and 0.5 µg SUR1 or 0.8 µg hKir2.1. Transfection mixtures were incubated for 1.5 h at room temperature and then added to each corresponding well. Mutations in both mKir6.2 and hKir2.1 were introduced using the QuikChange II method (Agilent Technologies), and the entire coding region was verified by sequencing.

Electrophysiology

Cells at 70–90% confluency were used for electrophysiological experiments, 24–48 h after transfection, with electrodes pulled from glass capillaries with a final resistance of 1.0–2.5 MΩ. All experiments were performed using a symmetrical high-potassium pipette and bath solution (K_{int}) consisting of (mM) 140 KCl, 1 EGTA, 1 K_2-EDTA, and 4 K_2HPO_4 and adjusted to pH 7.4 (KOH). Glass coverslips plated with transfected cells were first broken into shards and placed in an oil-gate perfusion chamber (Lederer and Nichols, 1989). Fluorescent cells expressing GFP were selected for patch clamp experiments. Current responses were low-pass filtered at 1 kHz (Axopatch 1B), sampled at 5–10 kHz (Digidata 1200), converted to digital files in Clampex7 (Molecular Devices), and stored on an external hard drive for offline analyses.

Patches were excised into zero ATP solutions, and K_{ATP} channel currents were recorded with a gap-free continuous voltage-clamp protocol (−50 mV membrane potential). WT K_{ATP} channel activity is characterized by a stable steady-state current response; however, over time the current slowly runs down. This process is correlated with the loss of inner leaflet membrane PIP_2 through diffusion or hydrolysis by various phosphatases and can be minimized by including divalent ion chelators in the recording solutions (Hilgemann and Ball, 1996; Ribalet et al., 2000). To minimize rundown, EDTA was therefore included in all phosphate-buffered K_{int} recording solutions used throughout these experiments.

ATP (Sigma-Aldrich) solutions were prepared daily from 200 mM stocks in K_{int} (pH 7.4, KOH) and stored at −20°C. Working stocks of 5 µg/ml (4.8 µM) porcine brain PIP_2 (Avanti Polar Lipids, Inc.) in K_{int} were stored at −80°C and sonicated on ice for 20 min before daily use.

Kir2.1 PIP_2 potentiation experiments were performed with a continually repeating voltage ramp protocol (holding potential 0 mV, ramp from −100 to 100 mV potential over 1 s). Current responses were elicited first in the cell-attached configuration, during patch excision into the inside-out configuration, and then, after loss of rectification, during subsequent application of PIP_2. Leak conductance was assessed at the end of each recording by the degree of residual current at −100 mV after application of 10 µM spermine (Fluka). [PIP_2] responses were assessed with a gap-free continuous voltage-clamp protocol at −100 mV. After excision, the patch was briefly exposed to a 10 mM $CaCl_2$ K_{int} solution to deplete endogenous PIP_2 before application of 1,2-dioctanoyl-*sn*-glycero-3-phospho-(1′-myo-inositol-4′,5′-bisphosphate) (DiC8-PIP_2; Avanti Polar Lipids, Inc.; prepared daily from a 100 µM stock stored at −80°C) K_{int} solution of varying concentrations. A high concentration (5 µg/ml) of brain PIP_2 was applied at the end of the recording to determine the maximum current response.

Homology modeling

A homology model of mKir6.2 was built using MODELLER9.8 (Eswar et al., 2007) using chicken Kir2.2 (cKir2.2; PDB ID 3SPI) as a template (Hansen et al., 2011). A pairwise sequence alignment was performed using Clust-

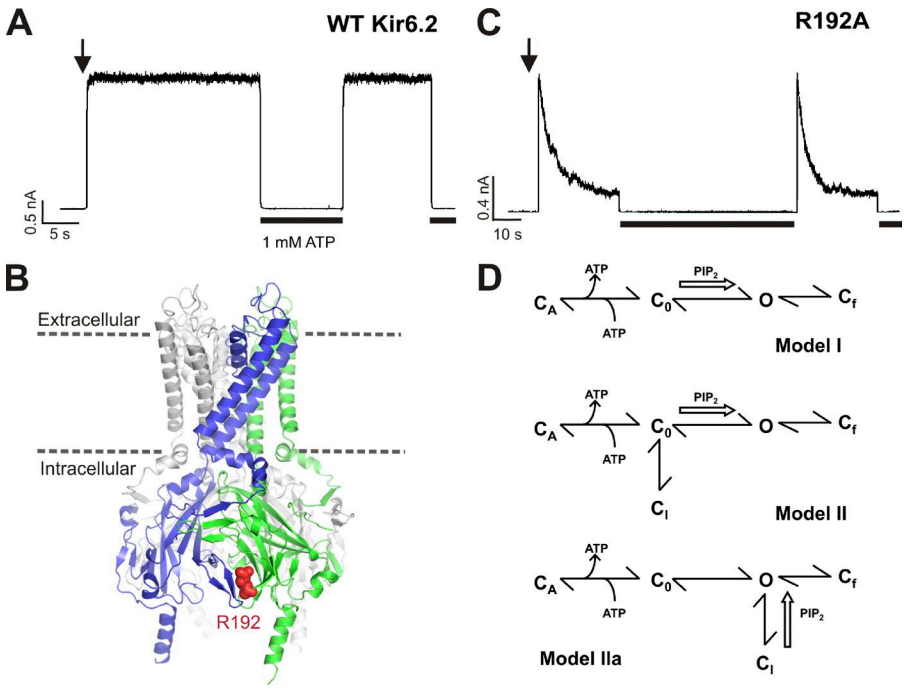

Figure 1. **K_{ATP} channel gating and inactivation.** (A) After patch excision, WT Kir6.2/SUR1 (K_{ATP}) channel currents activate to a stable level and are reversibly inhibited by application of 1 mM cytoplasmic ATP (black line). In this panel and in C, the arrow indicates patch excision. (B) Tetrameric Kir6.2 homology model depicting R192 (red) located at the CD-I between adjacent subunits (blue and green). (C) Kir6.2[R192A] channels are inhibited by ATP and then exhibit activation followed by fast current decay after removal of ATP. (D) Simplified models of K_{ATP} channel gating consisting of a closed apo (C_0) state, ATP-bound stabilized closed (C_A) state, inactivated (C_I) state, PIP_2-bound stabilized open (O) state, and short-lived closed flicker (C_f) state.

alW2 (Sievers et al., 2011), and 50.6% sequence identity was observed when compared for the region structurally resolved in the cKir2.2 crystal structure (cKir2.2: 43–372; mKir6.2:33-359). A tetrameric cKir2.2 structure was generated using PyMOL (PyMOL Molecular Graphics System, version 1.8; Schrödinger, LLC), and the tetramer was used to build a tetrameric mKir6.2 homology model.

Data analyses

Inactivation parameters. K_{ATP} channel inactivation parameters were evaluated as follows. The remaining current after inactivation was calculated as the ratio of steady-state (I_{ss}) to peak (I_{pk}) current (I_{ss}/I_{pk}) after ATP removal, and extent of inactivation was calculated as ($1 - I_{ss}/I_{pk}$). The time course of inactivation (τ_{inact}) was determined by fitting a mono-exponential function, $A(t) = A_1 e^{-t/\tau}$, to the current decay phase, in Clampfit (Clampfit 10.3 software; Molecular Devices). The degree of PIP_2 potentiation was calculated from the final current in zero ATP (I_{max}) after application of PIP_2, and the initial current in zero ATP ($I_{initial}$), before PIP_2 application, for both I_{pk} (I_{pk} PIP_2 potentiation) and I_{ss} (I_{ss} PIP_2 potentiation) current amplitude after patch excision: PIP_2 potentiation = $[I_{max} - I_{initial}]/I_{initial}$.

Single-channel recordings. Preprocessing and analyses were performed offline with QuB kinetic and statistical software (University at Buffalo, Buffalo, NY). Individual traces were preprocessed to correct for instances of baseline drift and infrequent noise spikes. Single-channel amplitudes were first estimated and fit with the "Amps" function, and the corresponding closed and open amplitudes were idealized with a 50% threshold method with no imposed dead time (Qin, 2004). Idealized data were segmented by the number of active channels, and only single-channel bursts were used for state and kinetic modeling. Simple 1 open (O) and 2–4 closed (C) state models ($C_{n+2} \leftrightarrow C_{n+1} \leftrightarrow C_n \leftrightarrow O \leftrightarrow C_f$) were constructed and used to fit the open interval distributions and to estimate mean open times (MOTs) and transitions rate constants ($O \rightarrow C_f$, k_{+Cf}; $C_f \rightarrow O$, k_{-Cf}; and $O \rightarrow C_n$, k_{-1}) using the maximum interval likelihood (MIL) algorithm in QuB with an imposed 0.4-ms dead time for each individual recording (Qin et al., 1996, 1997; Qin and Li, 2004).

Stationary noise analysis. 1-s segments of K_{ATP} channel currents recorded at −50 mV in zero and 1 mM ATP were used to estimate open probability (P_o) in zero ATP ($P_{o,zero}$) from individual macroscopic current recordings containing an unknown number of channels (N) with Eq.1:

$$P_{o,zero} = 1 - \frac{\sigma^2}{Ii}, \quad (1)$$

where I is the mean current in zero ATP − mean current in 1 mM ATP, σ^2 is the difference in the mean variance measured at zero and 1 mM ATP, and i is the single-channel amplitude (3.75 pA; Shyng et al., 1997a; Enkvetchakul et al., 2000).

Kir2.1 PIP_2 potentiation. The degree of potentiation of Kir2.1 currents by PIP_2 was calculated as the fold increase of the excised current amplitude (at −100 mV) after application of PIP_2. The DiC8-PIP_2 dose–response was fitted in OriginPro by Eq. 2:

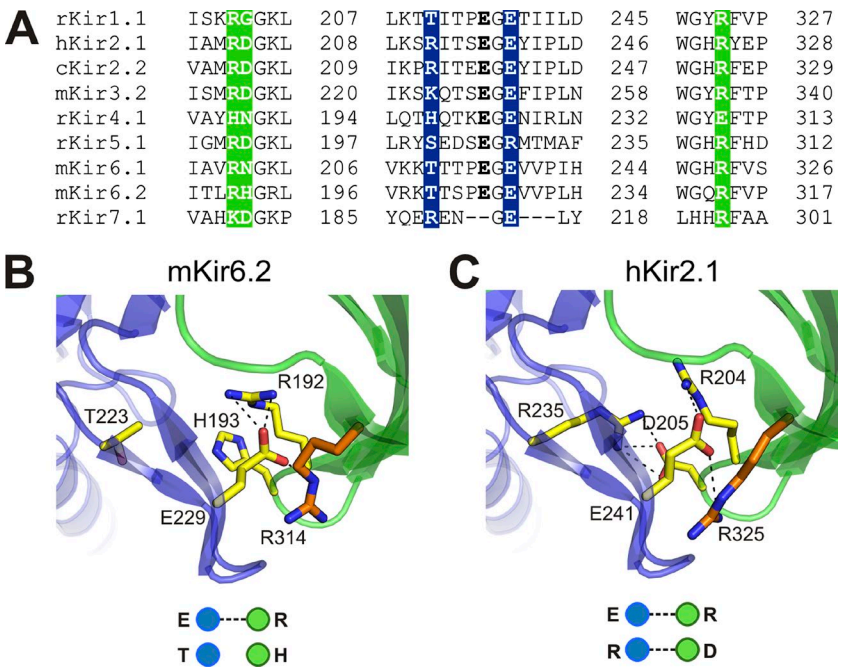

Figure 2. **Conserved and unique salt bridge interactions at the CD-I in Kir channels.** (A) Sequence alignment of eukaryotic Kir channel residues in the cytoplasmic domain. Charged residues that form intersubunit CD-I interactions are highlighted and colored with respect to their subunit orientation. (B and C) Homology models of mouse Kir6.2 (mKir6.2; B) and human Kir2.1 (hKir2.1; C) with adjacent subunits individually colored (blue and green) and cartoon representation of intersubunit interactions (R192–E229 in mKir6.2 and R204–E241 and D205–R235 in hKir2.1).

$$\frac{I_{DiC8}}{I_{PIP2}} = \left\{1 + \left(\frac{EC_{50}}{[DiC8]}\right)^{n_H}\right\}^{-1}, \quad (2)$$

where

$$\frac{I_{DiC8}}{I_{PIP2}}$$

is the current (I_{DiC8}) at defined concentration of DiC8-PIP_2 [*DiC8*] normalized to the maximum PIP_2 potentiated current (I_{PIP2}), EC_{50} is the half-maximal effective DiC8-PIP_2 concentration, and n_H is the Hill coefficient.

Statistics. Values are reported as mean ± SEM, and differences were evaluated with a two-tail Student's *t* test and were considered significant for $P < 0.05$.

RESULTS

Neutralization of CD-I–positive charges induces K_{ATP} current inactivation

WT K_{ATP} channels display negligible activity in cell-attached patch-clamp configuration, being mostly inhibited by intracellular ATP. Patch excision relieves this inhibition, resulting in maintained channel activity that is reversibly inhibited by subsequent application and removal of ATP (Fig. 1 A). Neutralization of certain positively charged intracellular residues, including R192A located at the CD-I (Fig. 1 B), has previously been demonstrated to induce a rapid spontaneous current decay following channel activation after patch excision (Shyng et al., 2000). This inactivation phenomenon is repeatedly observed after subsequent application and removal of ATP (Fig. 1 C).

Various models of K_{ATP} channel activity have been proposed to describe both macroscopic and microscopic kinetic parameters and sensitivity to numerous ligands (Nichols and Lederer, 1991; Alekseev et al., 1997; Enkvetchakul et al., 2000; Proks et al., 2001). Although more complexity is required to account for detailed single-channel behavior, a simplified three-state model in which the unliganded closed state (C_0) can either bind ATP to stabilize the closed channel (C_A) or open (O) as a result of binding PIP_2 (Fig. 1 D, Model I) can adequately describe macroscopic channel properties (Enkvetchakul and Nichols, 2003). As discussed further below, addition of a fourth state, the closed inactivated (C_I) state, accessible from the C_0 state or perhaps the O state (see below; Fig. 1 D, Model II or IIa), can then account for the novel inactivating behavior exhibited by the R192A mutation (Loechner et al., 2011).

Residues responsible for K_{ATP} channel inactivation are conserved throughout Kir channels

A similar inactivating phenotype has been shown for mutations at residues R314 and E229 (Shyng et al., 2000; Lin et al., 2003). These residues are conserved across the Kir channel family (Fig. 2 A) and, although there is no available Kir6.2 crystal structure, homology models based on crystal structures of chicken Kir2.2 (cKir2.2) indicate that these residues are all located close to one another and form a network of intersubunit contacts (Fig. 2 B; Tao et al., 2009; Hansen et al., 2011). R314 as well as R192 from the same subunit is predicted to interact with E229 in the adjacent subunit. Human Kir2.1 (hKir2.1) contains the equivalent electrostatic contacts, as well as an additional salt bridge, that is not present in Kir6.2. This is formed by residue D205, located one residue below R204 (equivalent to the conserved Kir6.2[R192]) and R235 on the adjacent

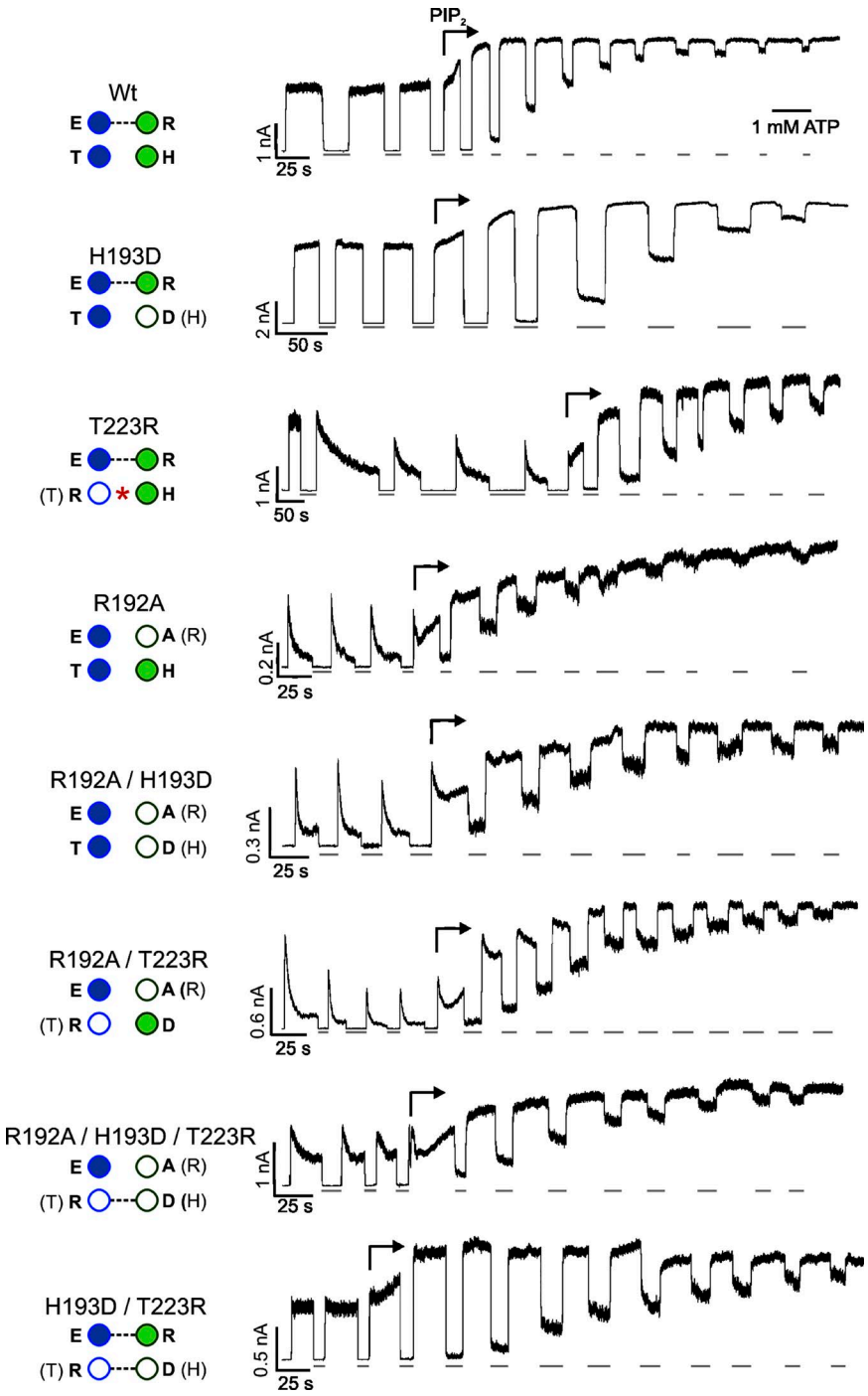

Figure 3. **Engineering unique Kir2.1 contacts into inactivating mutant Kir6.2 channels.** Macroscopic K_{ATP} channel current responses to ATP (1 mM, gray lines) in excised patches. Arrows indicate the first application of PIP_2 (5 μg/ml), which was then present for the remaining duration of the recording. * indicates potential repulsion between sidechains.

subunit (Fig. 2 C). The equivalent residues in Kir6.2 are H193 and T223, but their relatively short sidechains are predicted to be too distant to interact (Fig. 2 B).

Strength of CD-I contacts controls the extent and time course of inactivation

Neutralization of any member of the intersubunit salt bridge network between R192, E229, and R314 induces inactivation in Kir6.2 (Lin et al., 2003). This suggests that inactivation may result from a relative dissociation of the subunits from one another and leads us to specifically hypothesize that the strength of CD-I interactions will control the degree of channel inactivation. Thus, we predict that weaker CD-I interactions will result in a greater degree of channel inactivation and that, vice versa, stronger CD-I interactions between subunits could result in less inactivation.

To test this hypothesis, we examined gating in a series of Kir6.2 mutant channels in which we manipulated the number and location of CD-I salt bridges by mutagenesis. Fig. 3 shows representative recordings from this series of mutant channels. There is essentially no inacti-

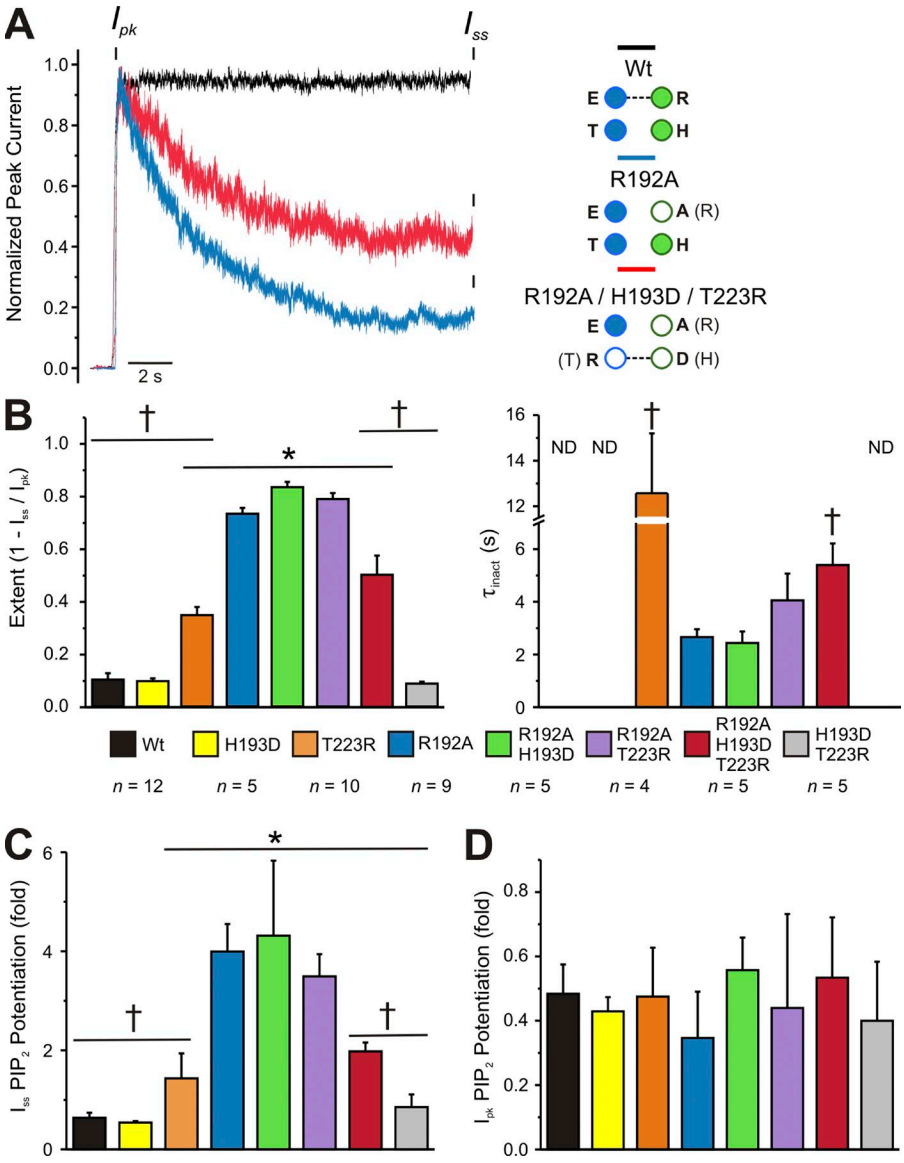

Figure 4. **The inactivating phenotype of Kir6.2[R192A] is rescued by introduced Kir2.1 CD-I contacts.** (A) Current response after initial patch excision of WT (black), R192A (blue), and R192A/H193D/T223R (red) channels, normalized to the peak current amplitude (I_{pk}). Steady-state current (I_{ss}) shows the extent of channel inactivation. (B) Extent ($1 - I_{ss}/I_{pk}$; left) and time course (τ_{inact}; right) of inactivation for CD-I mutations, from experiments as in Fig. 3. (C and D) Fold increase of steady-state (I_{ss}; C) and initial (I_{pk}; D) current amplitude after PIP_2 potentiation; means ± SEM; *, $P < 0.05$ relative to WT means; †, $P < 0.05$ relative to R192A means (Student's *t* test).

vation in mutants for which the endogenous R192–E229 salt bridge is preserved (e.g., H193D) or in which the additional salt bridge equivalent to the Kir2.1 D204–R235 interaction is introduced (e.g., H193D–T223R). However, in the absence of the H193D mutation, introduction of the T223R mutation itself causes inactivation, potentially caused by introduction of repulsive interaction between positively charged R223 and H193 sidechains. Significant inactivation is present in the R192A mutant, as well as R192A/H193D and R192A/T223R double mutants, in all of which the endogenous R192A-E229 salt bridge is broken. Importantly, both the extent and rate of inactivation resulting from R192A are markedly reduced by introduction of the second Kir2.1 equivalent salt bridge (H193D–T223R) in R192A/H193D/T223R channels. Inactivation parameters immediately after patch excision, and then degree of potentiation by PIP_2, were assessed for all CD-I mutants (Fig. 4). Channels containing the R192A mutation (R192A, R192A/H193D, and R192A/T223R) all exhibited >70% inactivation (Fig. 4, A and B). Inactivation of these channels was well fitted by a single exponential component with a time constant of inactivation (τ_{inact}) of 2–4 s. Importantly, introduction of the H193D–T223R salt bridge on the R192A background (in the triple R192A/H193D/T223R mutant) significantly reduced the extent of inactivation (to ~50%) and slowed τ_{inact} (to >5 s; Fig. 4, A and B).

The CD-I controls inactivation specifically, without affecting open state stability or ATP sensitivity

All Kir channels are activated by PIP_2, which shifts the open probability (P_o) to favor the O state. In WT Kir6.2 + SUR1 K_{ATP} channels, the P_o in zero [ATP] ($P_{o,zero}$) is typically ~0.4–0.6 (Inagaki et al., 1995; Trapp et al., 1998; Enkvetchakul et al., 2000, 2001; Ribalet et al.,

Table 1. **Single-channel properties of Kir6.2 CD-I mutations**

Construct	*n*	τ_o	τ_{Cf}	k_{+Cf}	k_{-Cf}	k_{-1}	Events analyzed	Total duration
		ms	*ms*	s^{-1}	s^{-1}	s^{-1}		*min*
WT	3	7.6 ± 0.4	0.32 ± 0.10	930 ± 50	5,970 ± 200	43 ± 5	2.1×10^5	34
R192A	4	7.8 ± 0.6	0.25 ± 0.07	890 ± 110	6,080 ± 80	46 ± 8	6.0×10^4	35
R192A/H193D/T223R	3	8.2 ± 0.4	0.30 ± 0.05	860 ± 60	6,010 ± 50	40 ± 4	5.1×10^4	18

Values are given as the rounded mean ± SEM.

2006). A simplified linear three-state model of K_{ATP} gating in which the channel exists in open (O), unliganded closed state (C_0), or closed ATP bound state (C_A) can account for reduced apparent sensitivity to ATP and a characteristic and very nonlinear relationship between apparent $K_{1/2,ATP}$ ([ATP] causing half-maximal inhibition) and $P_{o,zero}$ (Enkvetchakul et al., 2000, 2001; Enkvetchakul and Nichols, 2003), by PIP_2 acting to shift the $C_0 \leftrightarrow O$ equilibrium toward the O state (Fig. 1 D). Mutations that intrinsically stabilize the O state can be introduced at multiple locations, prominently in the pore of the channel (Loussouarn et al., 2000, 2001; Enkvetchakul et al., 2001), and these result in shifts along this same relationship (Enkvetchakul and Nichols, 2003). Inactivation might proceed from either the unliganded closed (C_0) or the open (O) state (Fig. 1 D). If

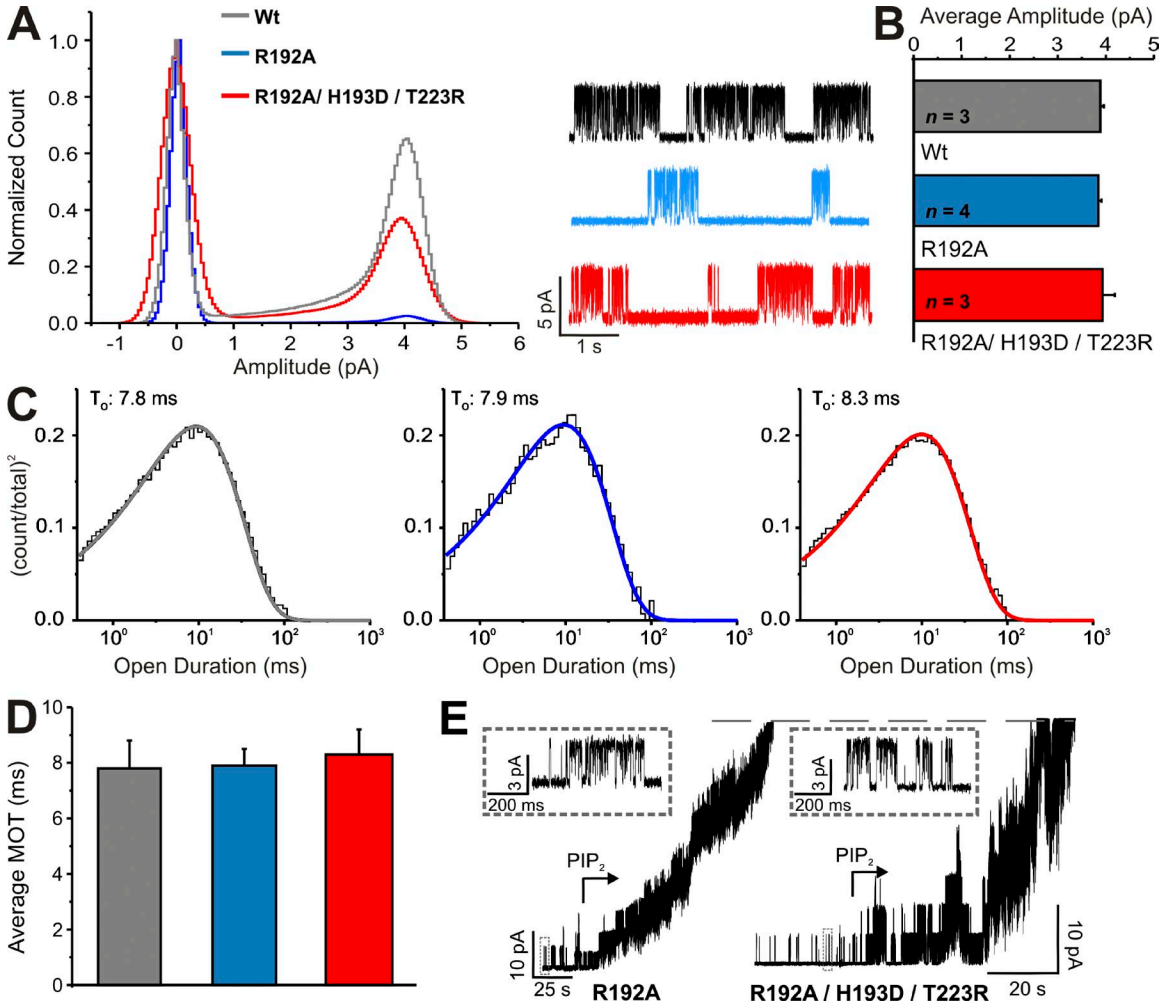

Figure 5. **CD-I strength does not contribute to the open state stability.** (A and B) Normalized single-channel amplitude histogram of the corresponding traces (right) for WT (gray), R192A (blue), and R192A/H193D/T223R (red) at −50 mV (A) and average single-channel amplitudes (B). (C) Open interval distributions overlaid with the probability density function (thick line) from the entire corresponding recordings depicted in A. (D) The open state time constant (τ_o, ms, inset) and average MOT (ms) were calculated from fits to unbiased models consisting of three to four closed states and one open state (see Materials and methods). (B and D) Means ± SEM. (E) Microscopic recordings of R192A (left) and R192A/H193D/T223R (right) before and after onset of PIP_2 application (arrows).

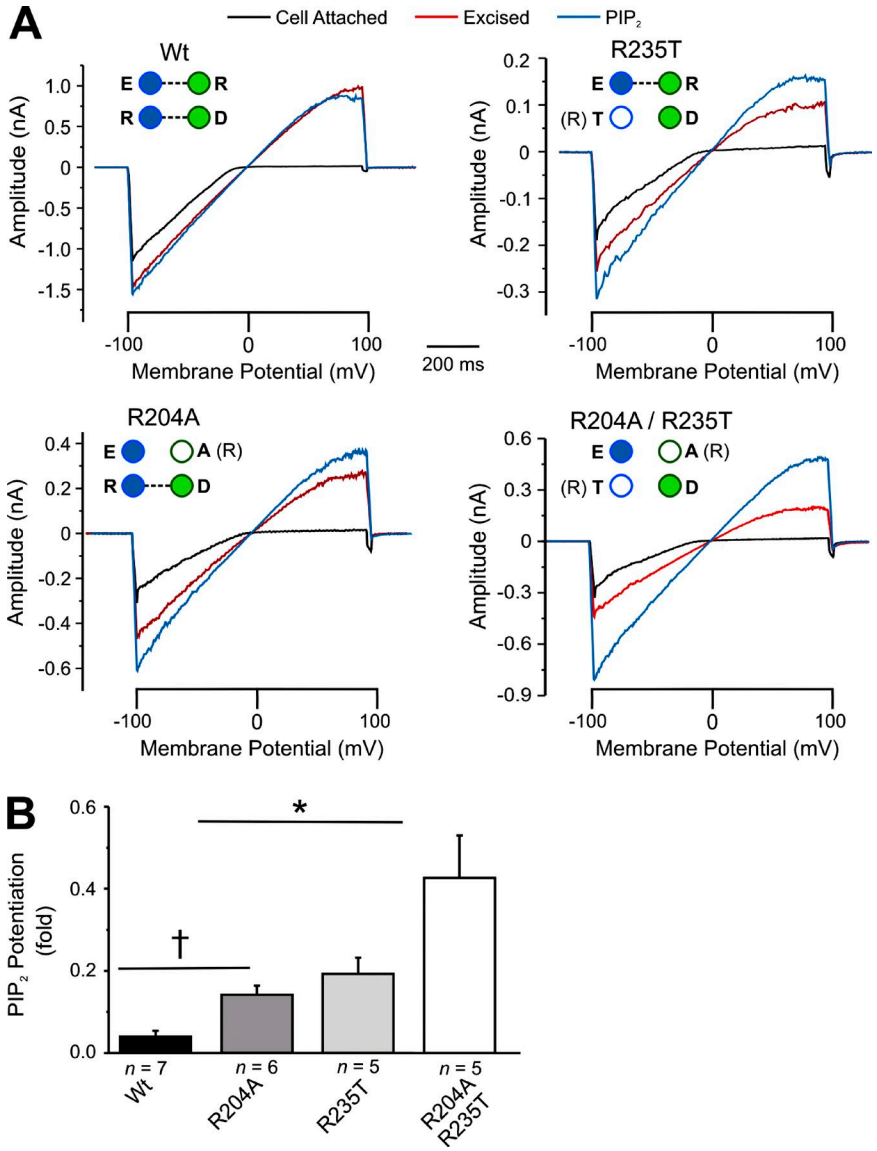

Figure 6. **Disruption of CD-I salt bridges reduces Kir2.1 channel activity.** (A) Current response to a 1-s voltage ramp from −100 to 100 mV. Currents were recorded in the cell-attached configuration (black), after patch excision (red), and after application of PIP_2 (5 µg/ml; blue). (B) PIP_2 potentiation of Kir2.1 channel excised currents; means ± SEM; *, $P < 0.05$ relative to WT means; †, $P < 0.05$ relative to R204A means (Student's *t* test).

the latter, then PIP_2 would also have to shift the $O \leftrightarrow C_I$ equilibrium toward the O state, but either model would then predict that application of PIP_2 will also decrease steady-state occupancy of the C_I state (i.e., the extent of inactivation) as the O state is stabilized. As can be seen from the recordings in Fig. 3, all mutant channels responded to PIP_2 as predicted, with not only profound loss of ATP sensitivity, but also loss of macroscopic inactivation. The potentiation of I_{ss} was ∼0.5-fold for WT channels but was more marked, essentially in proportion to the initial extent of inactivation, in the CD-I mutant channels (Fig. 4 C).

An important prediction of either model is that the inactivation process itself is independent of the intrinsic ATP-independent gating. Therefore, if CD-I mutations affect specifically the inactivation process, the $C_A \leftrightarrow C_0 \leftrightarrow O \leftrightarrow C_f$ equilibria should be unaffected. Given the kinetic separation between channel activation after ATP removal and the relatively slow inactivation, I_{pk} can provide an estimate of channel activation (i.e., $C_A \rightarrow C_0 \leftrightarrow O \leftrightarrow C_f$ transitions). As shown in Fig. 4 D, there was no significant difference in the degree of I_{pk} potentiation by PIP_2 (I_{pk} was potentiated ∼0.5-fold by PIP_2 for all mutations), implying that the initial peak $P_{o,zero}$ and hence channel activation transitions are the same for all channels. Consistent with this conclusion, $P_{o,zero}$ calculated from stationary noise analysis (Eq. 1) was not significantly different between WT (0.52 ± 0.05, $n = 6$) and H193D/T223R (0.45 ± 0.06, $n = 5$) channels, further indicating a similar $C_0 \leftrightarrow O \leftrightarrow C_f$ equilibrium.

Recordings from inside-out patches with resolvable single-channel openings revealed no significant difference in single-channel amplitudes (Fig. 5, A and B) nor MOTs between WT, R192A, or R192A/H193D/T223R channels (Fig. 5 D). There was no significant difference in the open state lifetime (Fig. 5 C) between WT and mutant channels, indicating that the strength of the CD-I interface does not contribute to the stability of the O

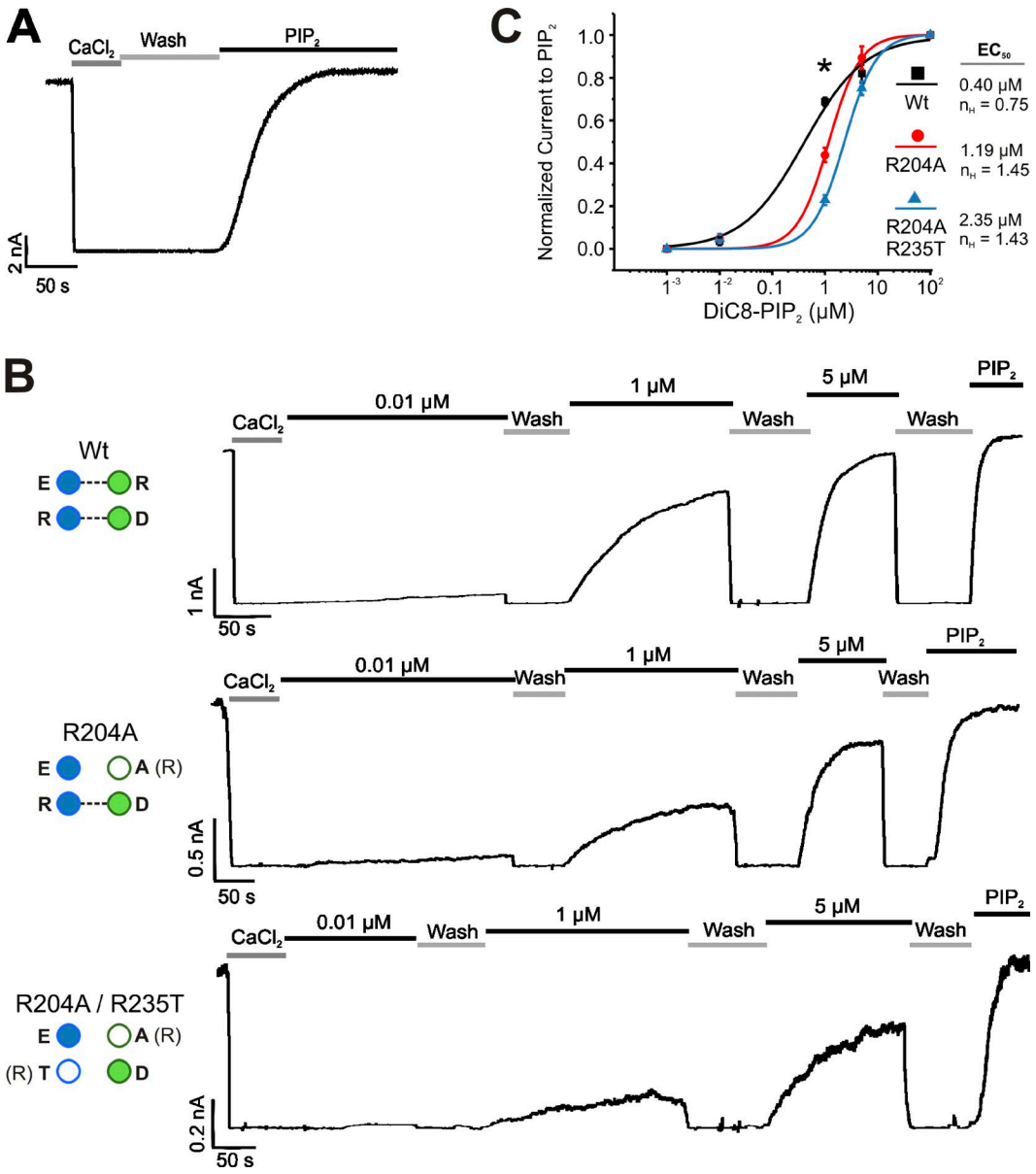

Figure 7. **Extent of Kir2.1 PIP_2 activation is controlled by CD-I stability.** (A) Depletion of endogenous PIP_2 with $CaCl_2$ (10 mM) eliminates channel activity, which is reactivated by application of exogenous PIP_2. (B) After $CaCl_2$ exposure, channel activity was measured at varying concentrations of short-chain PIP_2 (DiC8-PIP_2), and the maximum response was determined at the end of each recording with PIP_2. (C) DiC8-PIP_2 dose–response relationship fit with the Hill equation (Eq. 2). Data are presented as means ± SEM; *, $P < 0.05$ relative to WT means (Student's *t* test).

state (Table 1). WT Kir6.2/SUR1 channels display prolonged bursts of channel openings and brief high-frequency closures (Alekseev et al., 1998; Trapp et al., 1998; Enkvetchakul et al., 2000). Apparent burst lengths were shorter and prolonged closures were longer for both R192A and R192A/H193D/T223R channels in patches with only single openings detectable after patch excision. However, all such patches actually contained many more channels that were trapped in prolonged closures, as was obvious after application of PIP_2 (Fig. 5 E), and thus measurements of these prolonged closures would be underestimated and were not quantified.

Conserved and unique CD-I salt bridges also control Kir2.1 channel activity

Although mutations that disrupt the R192–E229 CD-I salt bridge in Kir6.2 cause an obvious inactivating phenotype in Kir6.2 channels, the consequences of similar mutations at equivalent residues in other Kir channels are not known. Kir2.1 channel gating is complex and not well characterized; channels exhibit one to four open conductance levels (Lu et al., 2001; Schwalbe et al., 2002; Amorós et al., 2013) and require binding of a secondary anionic phospholipid (PL) for activity (Lee et al., 2013). Lack of any rapid inhibitory ligands (i.e.,

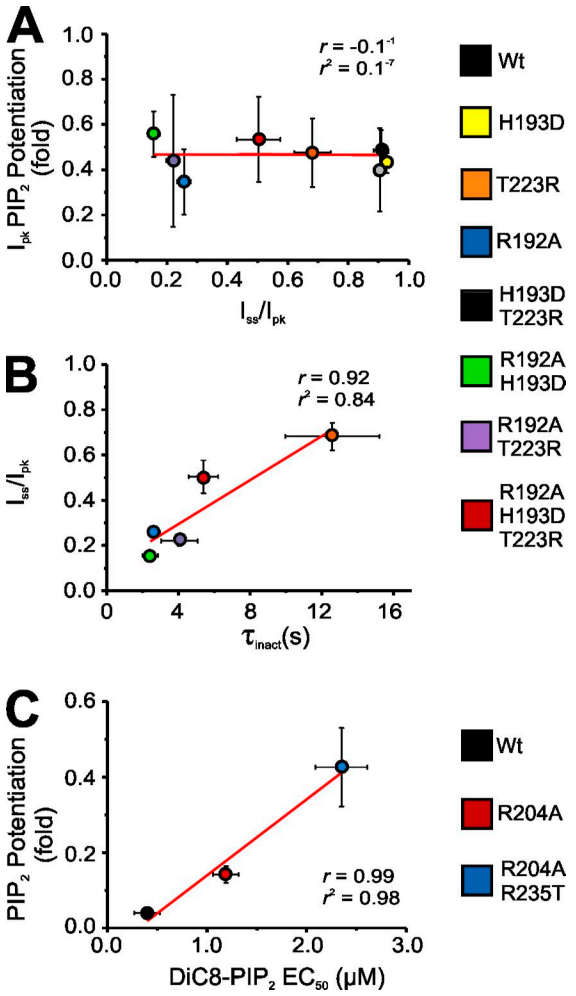

Figure 8. **Strength of the CD-I correlates with inactivation parameters.** (A and B) I_{pk} PIP_2 potentiation versus I_{ss}/I_{pk} (A) and I_{ss}/I_{pk} (B) for inactivating mutants versus τ_{inact}, for Kir6.2 CD-I mutations (data from Fig. 4). (C) Correlation between Kir2.1 PIP_2 potentiation and DiC8-PIP_2 EC_{50}. The corresponding correlation coefficient (r) and coefficient of determination (r^2) from each linear regression fit (red) are provided (inset). Data are presented as means ± SEM.

equivalent to ATP for Kir6.2) makes it impossible to directly assess any macroscopic inactivation. However, if we were to assume similar minimalistic gating models to those proposed for Kir6.2 (Fig. 1 D), but lacking the ATP-bound C_A state, occupancy of C_I in Kir2.1 would still be reflected in the degree of PIP_2 potentiation of steady-state current. WT, R204A, R235T, and R204A/R235T mutant Kir2.1 channel activity was assessed after the loss of polyamine-dependent rectification that occurs after patch excision (Fig. 6 A; Lopatin et al., 1994; Kurata et al., 2010). WT channel currents exhibited only minimal PIP_2 potentiation, consistent with a high intrinsic P_o, but the R204A mutation (which disrupts the R204–E241 salt bridge) resulted in significantly greater potentiation. Abolishing the D205–R235 salt bridge with the R235T mutation also resulted in greater PIP_2 potentiation, and these two effects were essentially additive in the R204A/R235T double mutation (Fig. 6, A and B). The change in degree of potentiation by PIP_2 indicates that the strength of the CD-I indeed also controls an underlying long closure in Kir2.1 channels.

Weakening the Kir2.1 channel CD-I lowers PIP_2 sensitivity

The consequence of a weaker CD-I on PIP_2 sensitivity was examined to further characterize the role of these contacts in Kir2.1 channel gating. Brief exposure to 10 mM $CaCl_2$ abolishes Kir2.1 channel currents by sequestering or depleting endogenous PIP_2 from excised patch membranes (Suh and Hille, 2008), such that channel activity can only be restored by subsequent application of exogenous PIP_2 (Fig. 7 A). To obtain a direct measure of sensitivity to PIP_2, the current recovery was measured by application of short chain DiC8-PIP_2, after $CaCl_2$-mediated PIP_2 depletion (Fig. 7 B). The DiC8-PIP_2 response relationship was fit with a modified Hill equation (Eq. 2). From such empirical fits, it is unclear whether the apparent change in slope is mechanistically meaningful, but the half-maximal DiC8-PIP_2 concentration (EC_{50}) calculated from the dose–response relationship (Eq. 2) significantly increased with the number of abolished CD-I contacts (Fig. 7 C).

DISCUSSION

Kir6.2 inactivation results from destabilization of the unliganded closed channel

Mutations of multiple residues in Kir6.2 (G156, R192, S208, S225, E229, V290, R301, and R314; Shyng et al., 2000; Lin et al., 2003, 2008, 2013; Loechner et al., 2011; Bushman et al., 2013) have now been shown to result in the distinct phenomenon whereby channel opening after removal of ATP is rapidly followed by channel closure. We have termed the phenomenon inactivation, by analogy to the closure of voltage-gated channels that follows channel activation in response to depolarization. All of these mutations, with the exception of G156, are located in or close to the CD-I (Fig. 9 A), and in each case, inactivation is attenuated as membrane PIP_2 levels are increased (Fig. 3; Shyng et al., 2000; Lin et al., 2003; Loechner et al., 2011; Bushman et al., 2013). WT Kir6.2 channel activity does not show any appreciable inactivation (Fig. 1 A) and can be modeled by assuming that each channel (or more accurately by assuming each subunit) exists in just three or four states (C_A, C_0, O, and C_f). Such models can account quantitatively for the very nonlinear change of apparent ATP sensitivity that occurs with change in $P_{o,zero}$, whether these are induced by mutations within the channel pore or by

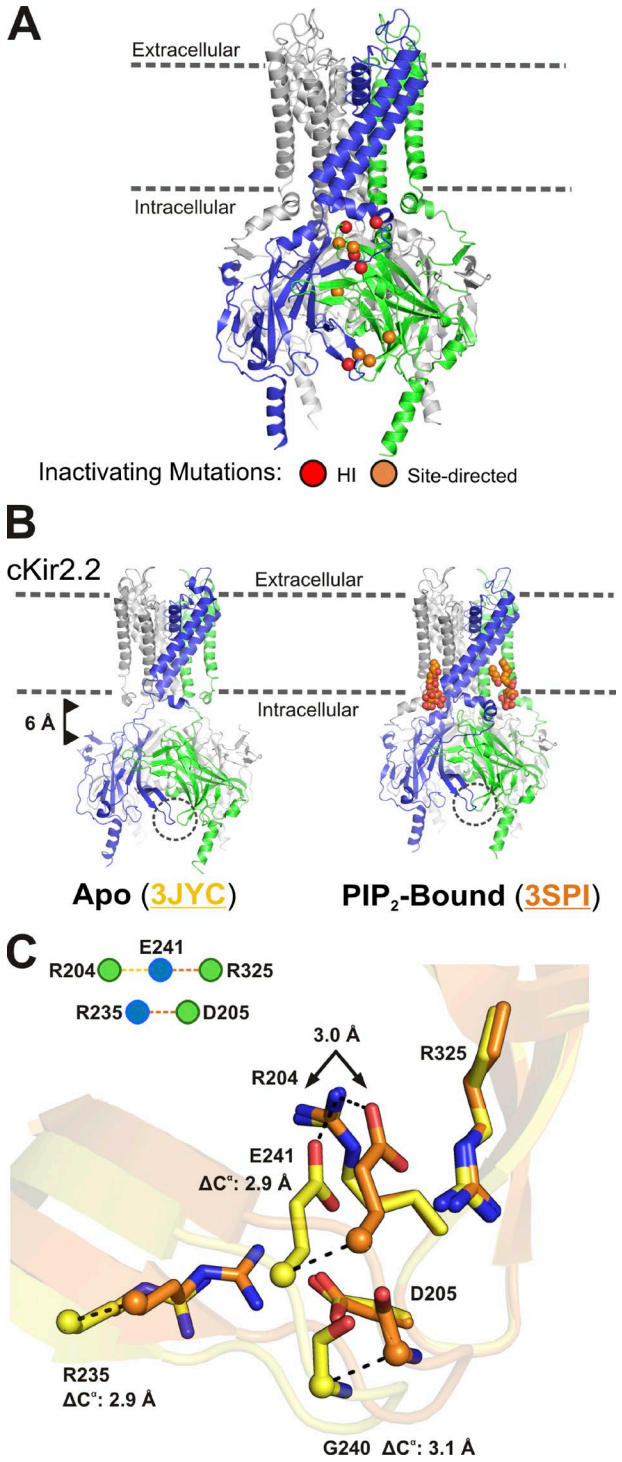

Figure 9. **PIP_2 binding to Kir2 is associated with CD-I rearrangements.** (A) Kir6.2 homology model with the location of CD-I residues that cause inactivation when mutated, whether identified in HI patients (red) or experimentally introduced (orange), indicated by spheres centered on the Cα position. (B) In the presence of PIP_2 (3SPI), the CD is ~6 Å closer to the membrane than in the apo cKir2.2 (3JYC) crystal structure. (C) Translocation of CD-I salt bridge residue C^{α} (ΔC^{α}) in 3JYC relative to 3SPI (structures aligned at R204). Only the R204–E241 salt bridge (3 Å) is preserved in 3JYC. The E241/R325 and D205/R235 intersubunit sidechain distances in 3JYC are beyond those necessary to form salt bridge contacts (residue numbering according to Kir2.1 sequence).

changing membrane PIP_2 levels (Trapp et al., 1998; Enkvetchakul et al., 2000, 2001). Inclusion of an additional C_I state, accessed from the unliganded C_0 state, can qualitatively explain inactivation (Enkvetchakul et al., 2001; Enkvetchakul and Nichols, 2003; Lin et al., 2003; Loechner et al., 2011). In the present paper, we have identified additional CD-I mutations that induce inactivation by breaking predicted salt bridges, as well as mutations that are predicted to introduce a novel salt bridge based on structural similarity to Kir2 channels (Fig. 2). Importantly, introduction of this salt bridge into inactivating Kir6.2 mutant channels slows and reduces the extent of inactivation.

Modeling Kir6.2 channel inactivation

The addition of an inactivated state is necessary to account for the macroscopic current decay after removal of ATP. Analysis of specific mutations indicates that they do not affect the apparent O state stability or the intraburst gating (i.e., the $C_0 \leftrightarrow O \leftrightarrow C_f$ equilibria; Fig. 5 and Table 1). These findings solidify the conclusion that the inactivation phenomenon is a reflection specifically of the transition to the C_I state and that mutations in the CD-I which induce the phenomenon (see below) are acting exclusively on this process, without affecting the stability of the "bundle crossing" gate that controls the $C_0 \leftrightarrow O$ equilibrium (Jiang et al., 2002). Consistent with this notion, Bushman et al. (2013) noted that, when PIP_2-dependent open state stability was substantially increased by addition of a second gain-of-function mutation, G156P inactivation was abolished. Conceivably, the inactivated (C_I) state could be accessed from either the unliganded C_0 state or the open (O) state. The experimental observations that (a) for different mutations, the greater the extent of inactivation, the faster the rate of inactivation (Fig. 8 B) and that (b) when PIP_2 is added, the rate of inactivation slows as the extent of inactivation decreases are readily accounted for by C_I being accessed from the unliganded closed state. If accessed from the open state, PIP_2 would have to act to slow the $O \rightarrow C_I$ transition. Moreover, if C_I were accessed from the open state, the reduced O to C_I rate would also prolong the open or the open burst time. Instead, we see reduction of the interburst intervals and, for this reason, favor the interpretation that C_I is accessed primarily from the C_0 state. However, realistic gating models of K_{ATP} activity are complex (Enkvetchakul et al., 2001; Enkvetchakul and Nichols, 2003; Proks and Ashcroft, 2009), and firm conclusions are difficult to draw.

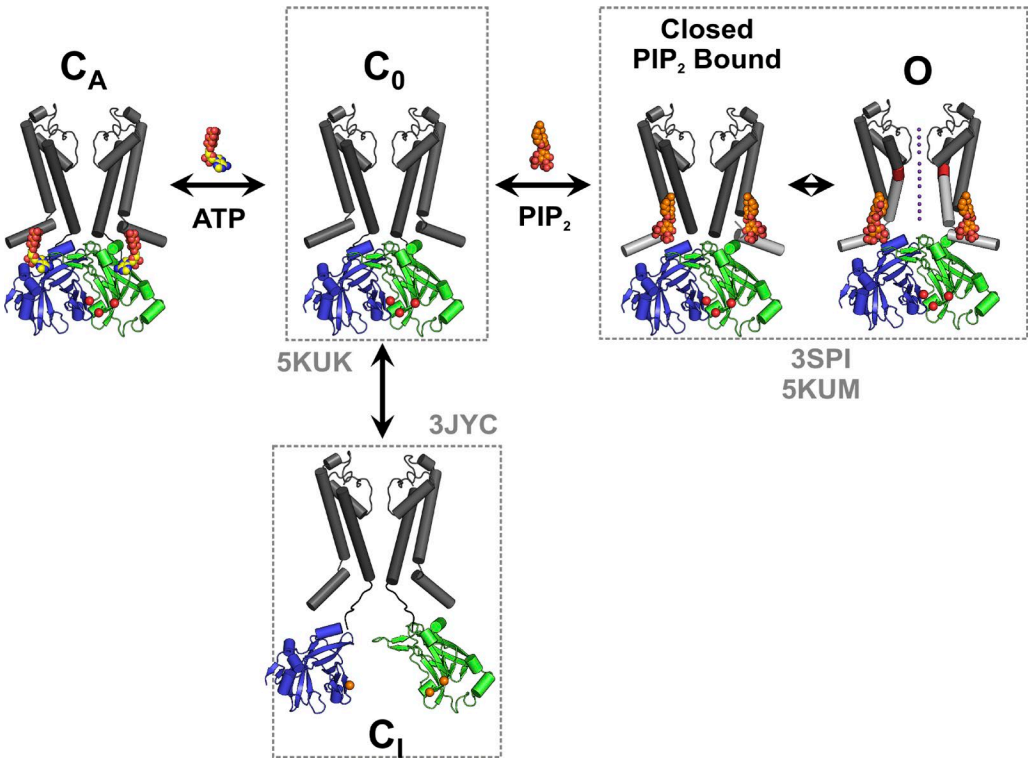

Figure 10. **Proposed model of K_{ATP} channel gating.** Cartoon model of proposed K_{ATP} channel gating states and inactivation caused by rupture of CD-I contacts, based on cKir2.2 structures. Stabilized CD-I interactions (red spheres) in the C_O channel (modeled on the K62W mutant 5KUK) permits binding of ATP or PIP_2 to transition to either ATP-bound (C_A) or PIP_2 bound (3SPI, 5KUM; O) states. Rupture of the CD-I contacts (orange spheres) disengages the CD from the membrane and results in transition to the apo (C_I; 3JYC) state, to which ligands cannot bind.

Kir6.2 inactivation results from destabilization of the CD-I, and the same gating process may be common to other Kir channels

Lin et al. (2003) first recognized that inactivation could be associated with breaking of salt bridges or charge networks at the CD-I. Here, we have confirmed the generality of this mechanism: breaking of the R192–E229 salt bridge results in Kir6.2 inactivation, and inactivation is reversed by introduction of the equivalent of the D205–R235 salt bridge found in Kir2.1. Importantly, breaking of either the D205–R235 or the R204–E241 salt bridges in Kir2.1 also results in decreased channel activity. WT Kir2.1 typically has a high P_o after patch excision (Lopes et al., 2002; Schwalbe et al., 2002), and there is minimal activation by subsequent addition of exogenous PIP_2 (Fig. 6 B). However, in Kir2.1[R204A] or in Kir2.1[R235T], basal channel activity is lower than WT, and the current is markedly potentiated after application of PIP_2 for both mutations (Fig. 6 B). Moreover, the extent of potentiation increases with the number of salt bridges broken; channel activity is even lower, and PIP_2 stimulation greater, in the R204A/R235T double mutation (Fig. 6 B). Without rapid activation gating driven by the dissociation of ATP, it is impossible to directly observe inactivation as a distinct macroscopic kinetic process in Kir2.1 channels, but the same gating scheme that describes Kir6.2 gating (but lacking the C_A state) could account for effects of salt bridge mutations on Kir2.1 gating. Thus, we suggest that the underlying molecular mechanism is likely common to both Kir6.2 and Kir2.1. Given the highly conserved nature of the Kir cytoplasmic domain structure (Fig. 2) and the presence of identical predicted or observed salt bridges in other members of the eukaryotic and prokaryotic Kir channel families (Kuo et al., 2003; Clarke et al., 2010; Hansen et al., 2011; Whorton and MacKinnon, 2011; Zubcevic et al., 2014; Linder et al., 2015), we predict that the mechanism may be common to all members.

What is the structural basis of inactivation?

The CD-I is not only bridged by charge networks in the protein itself, it is also the location of the binding site for PIP_2 in Kir channels (Hansen et al., 2011; Whorton and MacKinnon, 2011), as well as the nonspecific anionic lipid site in Kir2.1 (Lee et al., 2013, 2016) and the ATP-binding site in Kir6.2 (Enkvetchakul and Nichols, 2003; Trapp et al., 2003; Antcliff et al., 2005). The simple state model that we use to account for Kir channel gating thus suggests an appealing physical mechanism for the inactivation phenomenon. Clearly, inactivation and recovery are relatively slow processes occurring over seconds, which might suggest that a relatively large

protein motion is involved. Given that inactivation is induced and enhanced by breaking of salt bridges between subunits, we hypothesize that disruption of these salt bridges makes the unliganded C_0 state physically unstable, such that inactivation (reflecting the $C_0 \rightarrow C_I$ transition) might actually result from the CD-I essentially disconnecting. Because the inhibitory ATP-binding site is also located in the CD-I, ATP binding may also act to stabilize the connected CD-I (but with the channel closed, i.e., in the ATP-bound [C_A] state), such that after removal of ATP, the channel rapidly transitions from $C_A \rightarrow C_0 \rightarrow O$ states and reaches a pre–steady state before equilibrating with the C_I state. The lack of effect of inactivation-inducing mutations on either the degree of I_{pk} potentiation by PIP_2 or the O state stability is consistent with the finding that these mutations have no effect on channel activation (i.e., the $C_A \rightarrow C_0 \leftrightarrow O \leftrightarrow C_f$ transitions; Fig. 8 A). In the presence of high [ATP], channels will be gradually trapped in the absorbing C_A state as the CD-I undergoes spontaneous reconnection (i.e., as the subunit undergoes occasional transitions out of the C_I state) such that, macroscopically, channels will open and then inactivate after ATP addition and removal. The strong positive correlation between the residual noninactivating current and τ_{inact} (Fig. 8 B) is consistent with the major consequence of disruption of the CD-I being to specifically increase the rate constant for entry into the C_I state. Because PIP_2 also binds at the subunit interface, it may also intrinsically stabilize the "connected" CD-I, shifting the $C_0 \leftrightarrow O$ equilibrium toward the O state, thereby reducing the extent and rate of inactivation.

Two distinct Kir2 channel structures have thus far been identified crystallographically: one in the absence of PIP_2 (Tao et al., 2009), in which the PIP_2-binding site is unstructured, and one bound to PIP_2 (Hansen et al., 2011), in which the binding site is highly structured and the whole cytoplasmic domain is pulled closer toward the membrane surface (Fig. 9 B). Comparison of the CD-I in the apo (PDB ID 3JYC) and PIP_2-bound (PDB ID 3SPI) Kir2.2 structures indicates major differences in the disposition of the cytoplasmic domain relative to the transmembrane domain (Fig. 9 B): the whole cytoplasmic domain is displaced from the membrane ∼6 Å. This is accommodated by unfolding of the linkers between the cytoplasmic N and C termini, leading to unstructuring of the PIP_2-binding site. Close inspection also indicates subtle yet potentially significant differences in the CD-I itself: an alignment of both structures at R204 illustrates how the CD-I widens ∼3 Å in the apo conformation such that the R235–D205 and E241–R325 residue pairs no longer form contacts (Fig. 9 C). These structural changes are very consistent with the novel hypothesis that the apo (3JYC) structure, rather than representing channels in the unliganded C_0 state, is actually in the inactivated (C_I) conformation (Fig. 10). This could then explain both why PIP_2 cannot bind to the C_I state (because the PIP_2-binding site is unformed in this structure) and the role of CD-I salt bridge destabilization in enhancing the transition rate into the C_I state.

If the PIP_2-bound 3SPI and 5KUM structures represent the PIP_2-bound O and C_f states, and 3JYC represents the C_I state, the question then arises: what is the structure of the C_0 state? In addition to PIP_2, Kir2 channel activity normally requires additional binding of anionic PL at a distinct nonspecific site (Lee et al., 2013). We have recently identified additional cKir2.2 structures in which introduction of a tryptophan at the distinct "anionic lipid"–binding site mimics the anionic lipid-bound state and allows activation by PIP_2 in the absence of PL (Lee et al., 2016). The cytoplasmic domain is tightly tethered to the membrane surface, and the PIP_2-binding site is fully structured in cKir2.2[K62W] crystal structures, in both the absence (PDB ID 5KUK) and the presence of PIP_2 (PDB ID 5KUM; Lee et al., 2016). Moreover, the CD-I is closed, with the inter-charge distances at the CD-I being nearly identical to those in the 3SPI structure. We thus suggest that 5KUK, in which the cytoplasmic domain is tethered to the membrane and the PIP_2 site is formed but not occupied by PIP_2, may reflect the C_0 state (Fig. 10).

Parallels to glutamate receptor desensitization

Ionotropic glutamate receptors (iGluRs) are ancestrally related to K channels, with high structural similarity in the TM1 and TM2 transmembrane domains (M1 and M3 in iGluRs; Sobolevsky et al., 2009), although they are inserted in opposite orientation in the membrane, such that the extracellular bilobal ligand-binding domains (LBDs) are analogous to the intracellular cytoplasmic domains in Kir channels. There are evident parallels between the physical mechanism we propose for inactivation and the extensively studied structural mechanism of iGluR desensitization (Sobolevsky, 2015). The LBDs are dimerized in a back to back orientation, which allows the transduction of agonist induced LBD closure to open the channel gate. However, inherent strain in this conformation results in rupture of the LBD dimer interface, closing the channel while still bound to agonist (Kumar and Mayer, 2013). Recent cryo-EM structures of iGluRs in the resting, preopen, and desensitized states reveal that the structural rearrangements associated with desensitization involve larger domain movements of multiple intersubunit interfaces than previously thought (Dürr et al., 2014; Zhu et al., 2016). Direct evidence for or against the structural basis that we propose for Kir channel inactivation (Fig. 10) awaits further studies, but parallels between Kir channels and iGluRs might be a clue to a common role of intersubunit rearrangement in desensitization and inactivation in multiple ion channel families.

ACKNOWLEDGMENTS

This work was supported by the National Institutes of Health grants HL54171 and DK109407 (to C.G. Nichols). W.F. Borschel was supported by National Institutes of Health training grants DK007120-38, HL007275-35, and HL125241-01.

The authors declare no competing financial interests.

Author contributions: W.F. Borschel, S. Wang, and C.G. Nichols conceived the project. S. Lee performed structural homology modeling. W.F. Borschel carried out experiments. W.F. Borschel and C.G. Nichols analyzed the data and wrote the paper, which was edited by S. Wang and S. Lee.

Richard W. Aldrich served as editor.

Submitted: 28 October 2016
Revised: 29 December 2016
Accepted: 1 March 2017

REFERENCES

Alekseev, A.E., M.E. Kennedy, B. Navarro, and A. Terzic. 1997. Burst kinetics of co-expressed Kir6.2/SUR1 clones: comparison of recombinant with native ATP-sensitive K^+ channel behavior. *J. Membr. Biol.* 159:161–168. http://dx.doi.org/10.1007/s002329900279

Alekseev, A.E., P.A. Brady, and A. Terzic. 1998. Ligand-insensitive state of cardiac ATP-sensitive K^+ channels. Basis for channel opening. *J. Gen. Physiol.* 111:381–394. http://dx.doi.org/10.1085/jgp.111.2.381

Amorós, I., P. Dolz-Gaitón, R. Gómez, M. Matamoros, A. Barana, M.G. de la Fuente, M. Núñez, M. Pérez-Hernández, I. Moraleda, E. Gálvez, et al. 2013. Propafenone blocks human cardiac Kir2.x channels by decreasing the negative electrostatic charge in the cytoplasmic pore. *Biochem. Pharmacol.* 86:267–278. http://dx.doi.org/10.1016/j.bcp.2013.04.023

Antcliff, J.F., S. Haider, P. Proks, M.S. Sansom, and F.M. Ashcroft. 2005. Functional analysis of a structural model of the ATP-binding site of the K_{ATP} channel Kir6.2 subunit. *EMBO J.* 24:229–239. http://dx.doi.org/10.1038/sj.emboj.7600487

Bichet, D., F.A. Haass, and L.Y. Jan. 2003. Merging functional studies with structures of inward-rectifier K^+ channels. *Nat. Rev. Neurosci.* 4:957–967. http://dx.doi.org/10.1038/nrn1244

Bushman, J.D., J.W. Gay, P. Tewson, C.A. Stanley, and S.L. Shyng. 2010. Characterization and functional restoration of a potassium channel Kir6.2 pore mutation identified in congenital hyperinsulinism. *J. Biol. Chem.* 285:6012–6023. http://dx.doi.org/10.1074/jbc.M109.085860

Bushman, J.D., Q. Zhou, and S.L. Shyng. 2013. A Kir6.2 pore mutation causes inactivation of ATP-sensitive potassium channels by disrupting PIP_2-dependent gating. *PLoS One.* 8:e63733. http://dx.doi.org/10.1371/journal.pone.0063733

Clarke, O.B., A.T. Caputo, A.P. Hill, J.I. Vandenberg, B.J. Smith, and J.M. Gulbis. 2010. Domain reorientation and rotation of an intracellular assembly regulate conduction in Kir potassium channels. *Cell.* 141:1018–1029. http://dx.doi.org/10.1016/j.cell.2010.05.003

Drain, P., L. Li, and J. Wang. 1998. K_{ATP} channel inhibition by ATP requires distinct functional domains of the cytoplasmic C terminus of the pore-forming subunit. *Proc. Natl. Acad. Sci. USA.* 95:13953–13958. http://dx.doi.org/10.1073/pnas.95.23.13953

Dürr, K.L., L. Chen, R.A. Stein, R. De Zorzi, I.M. Folea, T. Walz, H.S. Mchaourab, and E. Gouaux. 2014. Structure and dynamics of AMPA receptor GluA2 in resting, pre-open, and desensitized states. *Cell.* 158:778–792. http://dx.doi.org/10.1016/j.cell.2014.07.023

Enkvetchakul, D., and C.G. Nichols. 2003. Gating mechanism of K_{ATP} channels: function fits form. *J. Gen. Physiol.* 122:471–480. http://dx.doi.org/10.1085/jgp.200308878

Enkvetchakul, D., G. Loussouarn, E. Makhina, S.L. Shyng, and C.G. Nichols. 2000. The kinetic and physical basis of K_{ATP} channel gating: toward a unified molecular understanding. *Biophys. J.* 78:2334–2348. http://dx.doi.org/10.1016/S0006-3495(00)76779-8

Enkvetchakul, D., G. Loussouarn, E. Makhina, and C.G. Nichols. 2001. ATP interaction with the open state of the K_{ATP} channel. *Biophys. J.* 80:719–728. http://dx.doi.org/10.1016/S0006-3495(01)76051-1

Eswar, N., B. Webb, M.A. Marti-Renom, M.S. Madhusudhan, D. Eramian, M.Y. Shen, U. Pieper, and A. Sali. 2007. Comparative protein structure modeling using MODELLER. *Curr. Protoc. Protein Sci.* Chapter 2:Unit 2.9.

Gloyn, A.L., E.R. Pearson, J.F. Antcliff, P. Proks, G.J. Bruining, A.S. Slingerland, N. Howard, S. Srinivasan, J.M. Silva, J. Molnes, et al. 2004. Activating mutations in the gene encoding the ATP-sensitive potassium-channel subunit Kir6.2 and permanent neonatal diabetes. *N. Engl. J. Med.* 350:1838–1849. http://dx.doi.org/10.1056/NEJMoa032922

Gribble, F.M., S.J. Tucker, and F.M. Ashcroft. 1997. The essential role of the Walker A motifs of SUR1 in K-ATP channel activation by Mg-ADP and diazoxide. *EMBO J.* 16:1145–1152. http://dx.doi.org/10.1093/emboj/16.6.1145

Hansen, S.B., X. Tao, and R. MacKinnon. 2011. Structural basis of PIP_2 activation of the classical inward rectifier K^+ channel Kir2.2. *Nature.* 477:495–498. http://dx.doi.org/10.1038/nature10370

Hibino, H., A. Inanobe, K. Furutani, S. Murakami, I. Findlay, and Y. Kurachi. 2010. Inwardly rectifying potassium channels: their structure, function, and physiological roles. *Physiol. Rev.* 90:291–366. http://dx.doi.org/10.1152/physrev.00021.2009

Hilgemann, D.W., and R. Ball. 1996. Regulation of cardiac Na^+,Ca^{2+} exchange and K_{ATP} potassium channels by PIP_2. *Science.* 273:956–959. http://dx.doi.org/10.1126/science.273.5277.956

Huang, C.L., S. Feng, and D.W. Hilgemann. 1998. Direct activation of inward rectifier potassium channels by PIP_2 and its stabilization by Gβγ. *Nature.* 391:803–806. http://dx.doi.org/10.1038/35882

Inagaki, N., T. Gonoi, J.P. Clement IV, N. Namba, J. Inazawa, G. Gonzalez, L. Aguilar-Bryan, S. Seino, and J. Bryan. 1995. Reconstitution of I_{KATP}: an inward rectifier subunit plus the sulfonylurea receptor. *Science.* 270:1166–1170. http://dx.doi.org/10.1126/science.270.5239.1166

Inagaki, N., T. Gonoi, J.P. Clement, C.Z. Wang, L. Aguilar-Bryan, J. Bryan, and S. Seino. 1996. A family of sulfonylurea receptors determines the pharmacological properties of ATP-sensitive K^+ channels. *Neuron.* 16:1011–1017. http://dx.doi.org/10.1016/S0896-6273(00)80124-5

Jiang, Y., A. Lee, J. Chen, M. Cadene, B.T. Chait, and R. MacKinnon. 2002. The open pore conformation of potassium channels. *Nature.* 417:523–526. http://dx.doi.org/10.1038/417523a

Koster, J.C., B.A. Marshall, N. Ensor, J.A. Corbett, and C.G. Nichols. 2000. Targeted overactivity of β cell K_{ATP} channels induces profound neonatal diabetes. *Cell.* 100:645–654. http://dx.doi.org/10.1016/S0092-8674(00)80701-1

Koster, J.C., M.S. Remedi, T.P. Flagg, J.D. Johnson, K.P. Markova, B.A. Marshall, and C.G. Nichols. 2002. Hyperinsulinism induced by targeted suppression of beta cell K_{ATP} channels. *Proc. Natl. Acad. Sci. USA.* 99:16992–16997. http://dx.doi.org/10.1073/pnas.012479199

Kumar, J., and M.L. Mayer. 2013. Functional insights from glutamate receptor ion channel structures. *Annu. Rev. Physiol.* 75:313–337. http://dx.doi.org/10.1146/annurev-physiol-030212-183711

Kuo, A., J.M. Gulbis, J.F. Antcliff, T. Rahman, E.D. Lowe, J. Zimmer, J. Cuthbertson, F.M. Ashcroft, T. Ezaki, and D.A. Doyle. 2003. Crystal structure of the potassium channel KirBac1.1 in the closed state. *Science.* 300:1922–1926. http://dx.doi.org/10.1126/science.1085028

Kurata, H.T., E.A. Zhu, and C.G. Nichols. 2010. Locale and chemistry of spermine binding in the archetypal inward rectifier Kir2.1. *J. Gen. Physiol.* 135:495–508. http://dx.doi.org/10.1085/jgp.200910253

Lederer, W.J., and C.G. Nichols. 1989. Nucleotide modulation of the activity of rat heart ATP-sensitive K^+ channels in isolated membrane patches. *J. Physiol.* 419:193–211. http://dx.doi.org/10.1113/jphysiol.1989.sp017869

Lee, S.J., S. Wang, W. Borschel, S. Heyman, J. Gyore, and C.G. Nichols. 2013. Secondary anionic phospholipid binding site and gating mechanism in Kir2.1 inward rectifier channels. *Nat. Commun.* 4:2786. http://dx.doi.org/10.1038/ncomms3786

Lee, S.J., F. Ren, E.M. Zangerl-Plessl, S. Heyman, A. Stary-Weinzinger, P. Yuan, and C.G. Nichols. 2016. Structural basis of control of inward rectifier Kir2 channel gating by bulk anionic phospholipids. *J. Gen. Physiol.* 148:227–237. http://dx.doi.org/10.1085/jgp.201611616

Lin, Y.W., T. Jia, A.M. Weinsoft, and S.L. Shyng. 2003. Stabilization of the activity of ATP-sensitive potassium channels by ion pairs formed between adjacent Kir6.2 subunits. *J. Gen. Physiol.* 122:225–237. http://dx.doi.org/10.1085/jgp.200308822

Lin, Y.W., J.D. Bushman, F.F. Yan, S. Haidar, C. MacMullen, A. Ganguly, C.A. Stanley, and S.L. Shyng. 2008. Destabilization of ATP-sensitive potassium channel activity by novel KCNJ11 mutations identified in congenital hyperinsulinism. *J. Biol. Chem.* 283:9146–9156. http://dx.doi.org/10.1074/jbc.M708798200

Lin, Y.W., A. Li, V. Grasso, D. Battaglia, A. Crinò, C. Colombo, F. Barbetti, and C.G. Nichols. 2013. Functional characterization of a novel KCNJ11 in frame mutation-deletion associated with infancy-onset diabetes and a mild form of intermediate DEND: a battle between K_{ATP} gain of channel activity and loss of channel expression. *PLoS One.* 8:e63758. http://dx.doi.org/10.1371/journal.pone.0063758

Linder, T., S. Wang, E.M. Zangerl-Plessl, C.G. Nichols, and A. Stary-Weinzinger. 2015. Molecular dynamics simulations of KirBac1.1 mutants reveal global gating changes of Kir channels. *J. Chem. Inf. Model.* 55:814–822. http://dx.doi.org/10.1021/acs.jcim.5b00010

Loechner, K.J., A. Akrouh, H.T. Kurata, C. Dionisi-Vici, A. Maiorana, M. Pizzoferro, V. Rufini, J. de Ville de Goyet, C. Colombo, F. Barbetti, et al. 2011. Congenital hyperinsulinism and glucose hypersensitivity in homozygous and heterozygous carriers of Kir6.2 (KCNJ11) mutation V290M mutation: K_{ATP} channel inactivation mechanism and clinical management. *Diabetes.* 60:209–217. http://dx.doi.org/10.2337/db10-0731

Lopatin, A.N., E.N. Makhina, and C.G. Nichols. 1994. Potassium channel block by cytoplasmic polyamines as the mechanism of intrinsic rectification. *Nature.* 372:366–369. http://dx.doi.org/10.1038/372366a0

Lopes, C.M., H. Zhang, T. Rohacs, T. Jin, J. Yang, and D.E. Logothetis. 2002. Alterations in conserved Kir channel-PIP_2 interactions underlie channelopathies. *Neuron.* 34:933–944. http://dx.doi.org/10.1016/S0896-6273(02)00725-0

Loussouarn, G., E.N. Makhina, T. Rose, and C.G. Nichols. 2000. Structure and dynamics of the pore of inwardly rectifying K_{ATP} channels. *J. Biol. Chem.* 275:1137–1144. http://dx.doi.org/10.1074/jbc.275.2.1137

Loussouarn, G., L.R. Phillips, R. Masia, T. Rose, and C.G. Nichols. 2001. Flexibility of the Kir6.2 inward rectifier K^+ channel pore. *Proc. Natl. Acad. Sci. USA.* 98:4227–4232. http://dx.doi.org/10.1073/pnas.061452698

Lu, T., L. Wu, J. Xiao, and J. Yang. 2001. Permeant ion-dependent changes in gating of Kir2.1 inward rectifier potassium channels. *J. Gen. Physiol.* 118:509–522. http://dx.doi.org/10.1085/jgp.118.5.509

Martin, G.M., P.C. Chen, P. Devaraneni, and S.L. Shyng. 2013. Pharmacological rescue of trafficking-impaired ATP-sensitive potassium channels. *Front. Physiol.* 4:386. http://dx.doi.org/10.3389/fphys.2013.00386

Nichols, C.G., and W.J. Lederer. 1991. The mechanism of KATP channel inhibition by ATP. *J. Gen. Physiol.* 97:1095–1098. http://dx.doi.org/10.1085/jgp.97.5.1095

Nichols, C.G., and A.N. Lopatin. 1997. Inward rectifier potassium channels. *Annu. Rev. Physiol.* 59:171–191. http://dx.doi.org/10.1146/annurev.physiol.59.1.171

Nichols, C.G., and M.S. Remedi. 2012. The diabetic β-cell: hyperstimulated vs. hyperexcited. *Diabetes Obes. Metab.* 14:129–135. http://dx.doi.org/10.1111/j.1463-1326.2012.01655.x

Nichols, C.G., S.L. Shyng, A. Nestorowicz, B. Glaser, J.P. Clement IV, G. Gonzalez, L. Aguilar-Bryan, M.A. Permutt, and J. Bryan. 1996. Adenosine diphosphate as an intracellular regulator of insulin secretion. *Science.* 272:1785–1787. http://dx.doi.org/10.1126/science.272.5269.1785

Proks, P., and F.M. Ashcroft. 2009. Modeling K_{ATP} channel gating and its regulation. *Prog. Biophys. Mol. Biol.* 99:7–19. http://dx.doi.org/10.1016/j.pbiomolbio.2008.10.002

Proks, P., C.E. Capener, P. Jones, and F.M. Ashcroft. 2001. Mutations within the P-loop of Kir6.2 modulate the intraburst kinetics of the ATP-sensitive potassium channel. *J. Gen. Physiol.* 118:341–353. http://dx.doi.org/10.1085/jgp.118.4.341

Qin, F. 2004. Restoration of single-channel currents using the segmental k-means method based on hidden Markov modeling. *Biophys. J.* 86:1488–1501. http://dx.doi.org/10.1016/S0006-3495(04)74217-4

Qin, F., and L. Li. 2004. Model-based fitting of single-channel dwell-time distributions. *Biophys. J.* 87:1657–1671. http://dx.doi.org/10.1529/biophysj.103.037531

Qin, F., A. Auerbach, and F. Sachs. 1996. Estimating single-channel kinetic parameters from idealized patch-clamp data containing missed events. *Biophys. J.* 70:264–280. http://dx.doi.org/10.1016/S0006-3495(96)79568-1

Qin, F., A. Auerbach, and F. Sachs. 1997. Maximum likelihood estimation of aggregated Markov processes. *Proc. Biol. Sci.* 264:375–383. http://dx.doi.org/10.1098/rspb.1997.0054

Remedi, M.S., J.V. Rocheleau, A. Tong, B.L. Patton, M.L. McDaniel, D.W. Piston, J.C. Koster, and C.G. Nichols. 2006. Hyperinsulinism in mice with heterozygous loss of K_{ATP} channels. *Diabetologia.* 49:2368–2378. http://dx.doi.org/10.1007/s00125-006-0367-4

Ribalet, B., S.A. John, and J.N. Weiss. 2000. Regulation of cloned ATP-sensitive K channels by phosphorylation, MgADP, and phosphatidylinositol bisphosphate (PIP_2): a study of channel rundown and reactivation. *J. Gen. Physiol.* 116:391–410. http://dx.doi.org/10.1085/jgp.116.3.391

Ribalet, B., S.A. John, L.H. Xie, and J.N. Weiss. 2006. ATP-sensitive K^+ channels: regulation of bursting by the sulphonylurea receptor, PIP_2 and regions of Kir6.2. *J. Physiol.* 571:303–317. http://dx.doi.org/10.1113/jphysiol.2005.100719

Schwalbe, R.A., C.S. Wingo, and S.L. Xia. 2002. Mutations in the putative pore-forming segment favor short-lived wild-type Kir2.1 pore conformations. *Biochemistry.* 41:12457–12466. http://dx.doi.org/10.1021/bi026304a

Shimomura, K., S.E. Flanagan, B. Zadek, M. Lethby, L. Zubcevic, C.A. Girard, O. Petz, R. Mannikko, R.R. Kapoor, K. Hussain, et al. 2009. Adjacent mutations in the gating loop of Kir6.2 produce neonatal diabetes and hyperinsulinism. *EMBO Mol. Med.* 1:166–177. http://dx.doi.org/10.1002/emmm.200900018

Shyng, S., and C.G. Nichols. 1997. Octameric stoichiometry of the K_{ATP} channel complex. *J. Gen. Physiol.* 110:655–664. http://dx.doi.org/10.1085/jgp.110.6.655

Shyng, S.L., and C.G. Nichols. 1998. Membrane phospholipid control of nucleotide sensitivity of K_{ATP} channels. *Science.* 282:1138–1141. http://dx.doi.org/10.1126/science.282.5391.1138

Shyng, S., T. Ferrigni, and C.G. Nichols. 1997a. Control of rectification and gating of cloned K_{ATP} channels by the Kir6.2 subunit. *J. Gen. Physiol.* 110:141–153. http://dx.doi.org/10.1085/jgp.110.2.141

Shyng, S., T. Ferrigni, and C.G. Nichols. 1997b. Regulation of K_{ATP} channel activity by diazoxide and MgADP. Distinct functions of the two nucleotide binding folds of the sulfonylurea receptor. *J. Gen. Physiol.* 110:643–654. http://dx.doi.org/10.1085/jgp.110.6.643

Shyng, S.L., C.A. Cukras, J. Harwood, and C.G. Nichols. 2000. Structural determinants of PIP_2 regulation of inward rectifier K_{ATP} channels. *J. Gen. Physiol.* 116:599–608. http://dx.doi.org/10.1085/jgp.116.5.599

Shyng, S.-L., J.D. Bushman, E.B. Pratt, and Q. Zhou. 2012. Molecular defects of ATP-sensitive potassium channels in congenital hyperinsulinism. *In* Monogenic Hyperinsulinemic Hypoglycemia Disorders. C.A. Stanley, and D.D. De Leoìn, editors. Karger, Basel. 30–42. http://dx.doi.org/10.1159/000334485

Sievers, F., A. Wilm, D. Dineen, T.J. Gibson, K. Karplus, W. Li, R. Lopez, H. McWilliam, M. Remmert, J. Söding, et al. 2011. Fast, scalable generation of high-quality protein multiple sequence alignments using Clustal Omega. *Mol. Syst. Biol.* 7:539. http://dx.doi.org/10.1038/msb.2011.75

Sobolevsky, A.I. 2015. Structure and gating of tetrameric glutamate receptors. *J. Physiol.* 593:29–38. http://dx.doi.org/10.1113/jphysiol.2013.264911

Sobolevsky, A.I., M.P. Rosconi, and E. Gouaux. 2009. X-ray structure, symmetry and mechanism of an AMPA-subtype glutamate receptor. *Nature.* 462:745–756. http://dx.doi.org/10.1038/nature08624

Suh, B.C., and B. Hille. 2008. PIP_2 is a necessary cofactor for ion channel function: how and why? *Annu. Rev. Biophys.* 37:175–195. http://dx.doi.org/10.1146/annurev.biophys.37.032807.125859

Tao, X., J.L. Avalos, J. Chen, and R. MacKinnon. 2009. Crystal structure of the eukaryotic strong inward-rectifier K^+ channel Kir2.2 at 3.1 Å resolution. *Science.* 326:1668–1674. http://dx.doi.org/10.1126/science.1180310

Trapp, S., P. Proks, S.J. Tucker, and F.M. Ashcroft. 1998. Molecular analysis of ATP-sensitive K channel gating and implications for channel inhibition by ATP. *J. Gen. Physiol.* 112:333–349. http://dx.doi.org/10.1085/jgp.112.3.333

Trapp, S., S. Haider, P. Jones, M.S. Sansom, and F.M. Ashcroft. 2003. Identification of residues contributing to the ATP binding site of Kir6.2. *EMBO J.* 22:2903–2912. http://dx.doi.org/10.1093/emboj/cdg282

Whorton, M.R., and R. MacKinnon. 2011. Crystal structure of the mammalian GIRK2 K^+ channel and gating regulation by G proteins, PIP_2, and sodium. *Cell.* 147:199–208. http://dx.doi.org/10.1016/j.cell.2011.07.046

Zhang, H., C. He, X. Yan, T. Mirshahi, and D.E. Logothetis. 1999. Activation of inwardly rectifying K^+ channels by distinct PtdIns(4,5)P_2 interactions. *Nat. Cell Biol.* 1:183–188.

Zhu, S., R.A. Stein, C. Yoshioka, C.H. Lee, A. Goehring, H.S. Mchaourab, and E. Gouaux. 2016. Mechanism of NMDA receptor inhibition and activation. *Cell.* 165:704–714. http://dx.doi.org/10.1016/j.cell.2016.03.028

Zubcevic, L., V.N. Bavro, J.R. Muniz, M.R. Schmidt, S. Wang, R. De Zorzi, C. Venien-Bryan, M.S. Sansom, C.G. Nichols, and S.J. Tucker. 2014. Control of KirBac3.1 potassium channel gating at the interface between cytoplasmic domains. *J. Biol. Chem.* 289:143–151. http://dx.doi.org/10.1074/jbc.M113.501833